

International Journal of Modern Physics: Conference Series
 © World Scientific Publishing Company

Linearly polarized superluminal waves in pulsar winds

IOANNA ARKA

*Max Planck Institut für Kernphysik, Saupfercheckweg 1
 Heidelberg, 69117, Germany*
 and

*Institute de Planétologie et d'Astrophysique de Grenoble, UMR 5274
 BP 53 F-38041 GRENOBLE
 ioanna.arka@ujf-grenoble.fr*

JOHN G. KIRK

*Max Planck Institut für Kernphysik, Saupfercheckweg 1
 Heidelberg, 69117, Germany
 john.kirk@mpi-hd.mpg.de*

Received Day Month Year

Revised Day Month Year

Pulsar winds are the ideal environment for the study of non-linear electromagnetic waves. It is generally thought that a pulsar launches a striped wind, a magnetohydrodynamic entropy wave, where plasma sheets carried along with the flow separate regions of alternating magnetic field. But when the density drops below a critical value, or equivalently for distances from the pulsar greater than a critical radius, a strong superluminal wave can also propagate. In this contribution we discuss the conversion of the equatorial striped wind into a linearly polarized superluminal wave, and we argue that this mode is important for the conversion of Poynting flux to kinetic energy flux before the outflow reaches the termination shock.

Keywords: plasmas; waves; acceleration of particles; pulsars:general; stars: winds, outflows.

PACS numbers: 11.25.Hf, 123.1K

1. Introduction

Pulsar winds are relativistic outflows, consisting mainly of electrons and positrons. They are thought to be Poynting-flux dominated at launch, as quantified by the magnetization parameter σ which is the ratio of Poynting to kinetic energy flux, with $\sigma \gg 1$. Far away from the light cylinder, which is at radius $r_{LC} = c/\omega$ with ω the pulsar's rotational frequency, the magnetic field is predominantly toroidal with an amplitude falling as $1/r$ and reverses sign across a corrugated current sheet that separates the two magnetic hemispheres. The wind propagates radially as a transverse subluminal wave with speed equal to the bulk speed of the outflow, or equivalently Lorentz factor Γ . The opening angle around the equator of the region

of alternating magnetic field depends on the misalignment of the magnetic and rotational axes of the pulsar, denoted by α .

In the absence of dissipation, the wave propagates outwards from the light cylinder while remaining Poynting-dominated¹. However, after crossing the termination shock, the outflow's magnetization is low². Where and when conversion of Poynting flux to particle energy happens is still not clear. Magnetic reconnection in the current sheets separating regions of opposite magnetic field polarity in the wind is a possible dissipation mechanism, however this process is much too slow to account for the conversion in isolated pulsars like the Crab, unless the pair injection by the pulsar is much larger than generally assumed^{3–5}. Another possibility is driven reconnection at the termination shock, which has been demonstrated to dissipate the striped wind's alternating field efficiently in some cases. This, however, requires even higher particle injection rates than reconnection in the current sheets^{6–8}.

A solution can be provided in the form of non-linear superluminal waves, i.e. electromagnetic waves of large amplitude with phase speed $v_\phi > c$. These can propagate outside of a critical radius r_{cr} , at regions of lower particle density⁹ (as a contrast to the magnetohydrodynamic wind which needs a minimum particle density). The conversion of the striped wind to a superluminal mode is possible if r_{cr} is smaller than the shock radius.

In the following we will investigate non-linear superluminal waves of linear polarization, which are relevant in a region of opening angle α around the equator of a pulsar wind. We identify the superluminal modes into which a striped wind can convert by imposing "jump conditions" across the (thin) region where conversion happens. We will assume throughout that the waves can be considered as locally plane and purely transverse. These are excellent approximations far away from the light cylinder (at $\rho = r/r_{\text{LC}} \gg 1$). The radial direction, which is the direction of propagation of the wave, can be identified with the x -direction in a cartesian system of coordinates. The surviving field components are then E_y and B_z , corresponding to the azimuthal magnetic field and the polar electric field.

2. Transverse superluminal waves: the two-fluid approach

The equations governing the evolution of a cold, two-component plasma are the continuity equation and the equations of motion for each species, along with Maxwell's equations. We are looking for periodic solutions in a special frame of reference that propagates with velocity c^2/v_ϕ with respect to the laboratory frame (in the laboratory frame, which coincides with the pulsar frame, the wave phase speed is v_ϕ). We will call this special frame "homogeneous" or "H-frame". The advantage of this formulation is that in the H-frame all space dependence vanishes and only time dependence remains, and the phase is just $\omega_0 t$ with ω_0 the wave frequency¹⁰. From now on quantities in the H-frame will be unprimed, while quantities in the laboratory frame will be primed.

In the H-frame, the conservation of magnetic flux ($\nabla \cdot \mathbf{B} = 0$) is automatic, and

it can be seen immediately from Faraday's law that the magnetic field is constant. From Coulomb's law and the continuity equation we get $n_+\gamma_+ = n_-\gamma_-$, where a plus(minus) subscript denotes positrons(electrons). Furthermore, the Lorentz factors are equal $\gamma_+ = \gamma_-$ and the other components of the dimensionless four-velocity of the two species are related by:

$$u_{x+} = u_{x-} \quad u_{y+} = -u_{y-} \quad u_{z+} = -u_{z-} . \quad (1)$$

Because of these equations we can drop the subscripts and solve the system in terms of the positron fluid quantities. It can be shown¹¹ that all quantities can be expressed in terms of the electric field normalized to its largest amplitude $y = E/E_0$:

$$\gamma = \gamma_0 + 2\gamma_0(1 - y^2)/q \quad (2)$$

$$u_x = \sqrt{\gamma_0^2 - 1 + 4\gamma_0\lambda(1 - y)/q} \quad (3)$$

$$u_y = \pm \sqrt{\gamma^2 - u_x^2 - 1} \quad (4)$$

$$u_z = 0 . \quad (5)$$

In the above, quantities with a zero subscript express the initial condition at zero phase, and the field reaches its largest amplitude at phase zero, $y_0 = 1$. Also, $\lambda = B/E_0$ is the ratio of the (constant) magnetic field to the electric field amplitude, and q is double the ratio at phase zero of the energy density in the particles to that in the electric field:

$$q = \frac{32\pi mc^2 \gamma_0^2 n_0}{E_0^2} . \quad (6)$$

The electric field y can be computed from a first-order differential equation, which in the general case ($\lambda \neq 0$) has no solution in closed form and has to be numerically integrated. The phase-averaged values of the above quantities, then, can also be calculated numerically (for details see Ref. 12).

3. Conserved quantities

There are four conserved quantities in a pulsar wind, in the plane wave approximation. These are the phase-averaged x -components of the particle, energy, momentum and magnetic flux densities. We will denote the particle flux by $\langle J' \rangle$, while the energy and momentum flux densities are the $\langle T'^{01} \rangle$ and $\langle T'^{11} \rangle$ components of the combined stress-energy four-tensor of fields and particles. Finally, the magnetic flux density can be replaced (from Faraday's law) by the phase-averaged electric field, so that the last conserved quantity can be written as $\langle E' \rangle^2 / (4\pi)$.

From these four quantities we can construct three dimensionless ones, defined as

$$\mu = \frac{\langle T'^{01} \rangle}{mc \langle J' \rangle} \quad (7)$$

4 ARKA & KIRK

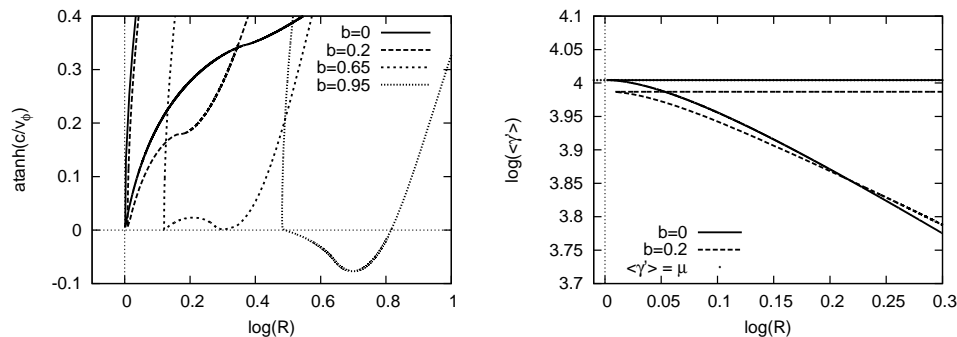


Fig. 1. On the left the index of refraction is plotted as a function of dimensionless radius R , for four different cases of b . On the right, the phase-averaged Lorentz factor of the particles is plotted. We see that for low b , $\langle \gamma \rangle \simeq \mu$, which means that almost the whole energy of the wind is now carried by the particle component of the flow.

$$\nu = \frac{\langle T'^{11} \rangle}{mc \langle J' \rangle} \quad (8)$$

$$\eta = \frac{\langle E' \rangle^2}{4\pi mc \langle J' \rangle}. \quad (9)$$

The first of these, μ , is the energy per unit mass that each particle would have, if the entire energy flux were carried by the particles. The three quantities (7)-(9) are conserved across a layer that marks the transition between the striped wind and the superluminal wave, and therefore they have to be expressed in terms of the quantities characterizing these modes. For the striped wind we have:

$$\mu = \Gamma(1 + \sigma) \quad (10)$$

$$\nu = [\Gamma^2(1 + \sigma) - (1 + \sigma/2)] (\Gamma^2 - 1)^{-1/2} \quad (11)$$

$$\eta = b^2 \Gamma \sigma \beta \quad (12)$$

where σ is the wind magnetization and b is the normalized DC component of the magnetic field. This quantity is zero at the equatorial plane, where regions of alternating field are equal in width and cancel out in the phase average, and rises to its maximum value, $b = 1$, at latitude equal to the inclination angle α , where the alternating field component disappears. The same quantities μ , ν and η can be calculated for the superluminal wave. Since our treatment of these modes took place in the H-frame, we calculate the quantities $\langle J \rangle$, $\langle T^{00} \rangle$, $\langle T^{01} \rangle$, $\langle T^{11} \rangle$ and $\langle E \rangle^2 / (4\pi)$ and transform them to the laboratory frame using the velocity c^2/v_ϕ , as explained above.

Equating Eqns. (7)-(9) calculated for the superluminal mode to Eqns. (10)-(12), one can find "jump conditions" for the transition from the striped wind to the superluminal mode, for certain values of Γ , σ and latitude, or equivalently b . We

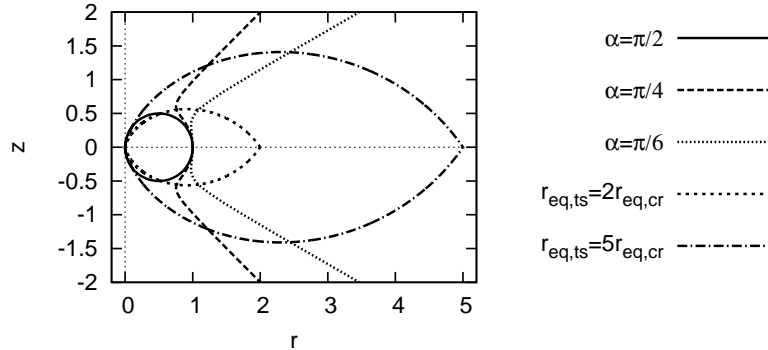


Fig. 2. The critical surfaces for three values of the inclination angle α , along with two example shock surface, normalized to equatorial radius $\rho_{\text{eq,ts}}$ two and five times larger than the equatorial critical radius $\rho_{\text{eq,cr}}$. The pulsar is at the point $(0, 0)$ and one half of the poloidal plane is shown. The variable r is normalized to the equatorial value of R .

can then re-introduce the conservation of particle flux into our system of equations, in order to find the radial dependence of these jump conditions¹².

4. Results and discussion

In Fig. 1 we have plotted as a function of normalized radius $R = \rho\mu/a_L$ the inverse hyperbolic tangent of the refractive index c/v_ϕ of the wave into which a striped wind with $\Gamma = 100$ and $\sigma = 100$ can convert. The quantity a_L is a dimensionless parameter given by:

$$a_L = \sqrt{\frac{4\pi\epsilon^2}{m^2c^5} \frac{dL}{d\Omega}} = a_{L0} \sin\theta, \quad (13)$$

where by $dL/d\Omega$ the distribution of the pulsar's luminosity in solid angle Ω is meant and θ is the colatitude (i.e. the polar angle). We have assumed that the distribution of the pulsar's luminosity follows the prescription

$$\frac{dL}{d\Omega} = L_0 \sin^2\theta \quad (14)$$

and separated the angular dependence from a_L .

As we can see in Fig. 1, there is a minimum normalized distance R_{cr} outside which superluminal waves can propagate. For $b = 0$, $R_{\text{cr}} \simeq 1$, but it rises as one goes to higher latitudes. On the plot on the right of Fig. 1 the phase averaged Lorentz factor of the particles, $\langle\gamma'\rangle$ is shown for the same values of b . From this plot it is seen that during the conversion from one wave to another, energy is transferred from fields to particles. In the striped wind the Lorentz factor of each particle is equal to the bulk Lorentz factor of the outflow, which in the plotted example is $\Gamma = 100 \ll \mu$.

However, in the superluminal wave, for low values of b , $\langle \gamma' \rangle \simeq \mu$, which means that almost all the energy of the outflow is now carried by particles. Even for values of b close to unity, $\langle \gamma' \rangle \gg \Gamma$, meaning that the particles get accelerated in the whole wind, and the ratio of the Poynting to the kinetic energy flux decreases during the transition from the subluminal to the superluminal regime.

In Fig. 2, the geometrical critical surface is shown (radius normalized as $\rho \rightarrow \rho\mu/a_{L0}$), outside which superluminal waves can propagate, for different values of the inclination α . Superimposed on the critical surfaces is the example of a shock surface, the shape of which is taken from Ref. 13. The normalization of the shock radius in comparison to the critical radius in Fig. 2 is arbitrary. Generally it depends on the individual pulsar in question. For isolated pulsars like the Crab and the Vela, the shock (located at $\sim 10^9 r_{LC}$ and $\sim 10^8 r_{LC}$ respectively¹⁴) is much farther out than the critical surface (located at $\sim 10^7 r_{LC}$ and $\sim 10^6 r_{LC}$ respectively) for practically the whole of the wind. For pulsars in binary systems, though, where the shock is pushed closer to the pulsar by the outflow from a companion star¹⁵, it is possible that the critical surface is partly or entirely outside the shock, so that no superluminal waves can propagate. In highly eccentric systems, the possibility arises that the termination shock migrates during one orbit from a location inside to one outside the critical surface, so that the characteristics of the wind just before the termination shock are orbitally modulated during one period of the system.

We conclude that the conversion of the striped wind to a superluminal mode is possible in many objects, especially in isolated pulsars, and it is accompanied by an acceleration of the particles of the outflow to $\langle \gamma' \rangle \gg \Gamma$, which might influence the physics of particle acceleration and the structure of the termination shock.

References

1. J. G. Kirk and I. Mochol, *Ap. J.* **729**, 104 (2011).
2. M. J. Rees and J. E. Gunn, *Mon. Not. R. Astron. Soc.* **167**, 1 (1974).
3. F. V. Coroniti, *Astron. Astroph.* **349**, 538 (1990).
4. Y. Lyubarsky and J. G. Kirk, *Ap. J.* **547**, 437 (2001).
5. J. G. Kirk and O. Skjaeraasen, *Ap. J.* **591**, 366 (2003).
6. Y. Lyubarsky, *Mon. Not. R. Astron. Soc.* **345**, 153 (2003).
7. Y. Lyubarsky and J. Petri, *Astron. Astroph.* **473**, 683 (2007).
8. L. Sironi and A. Spitkovsky, *Ap. J.* **741**, 39 (2011).
9. A. Melatos and D. B. Melrose, *Mon. Not. R. Astron. Soc.* **279**, 1168 (1996).
10. P. C. Clemmow, *J. Pl. Ph.* **12**, 297 (1974).
11. C. F. Kennel and R. Pellat, *J. Pl. Ph.* **15**, 335 (1976).
12. I. Arka and J. G. Kirk, *arXiv:1109.2756v1* (accepted for publication in *Ap. J.*) (2011).
13. Y. Lyubarsky, *Mon. Not. R. Astron. Soc.* **329**, L34 (2002).
14. O. Kargaltsev and G. G. Pavlov *eprint arXiv: 0801.2602v2*, (2009).
15. Chatterjee. S. et al, *Ap. J.* **x670**, 1301 (2007).